chaos (Fig. 2), confirm that the degree of cardiac chaos was decreased in the CHF patients.

These critical tests strongly support the suggested prevalence of cardiac chaos in healthy subjects[8,9]. Moreover, our results indicate that cardiac chaos persists in CHF patients, albeit less strongly than in healthy subjects. The intermittent heartbeat oscillations characteristic of these patients[22] (Fig. 1) suggest that they may be at the brink of intermittency, a common route to and out of chaos[25]. Whereas the effect of noise contamination of the data precluded the reliable detection of chaos with previous approaches, we have used this property to evaluate statistically the changes in cardiac chaos with heart disease. Such a statistical approach has been made possible by the sensitivity, specificity and computational efficiency of the chaotic test[19].

Our results do not reveal the mechanisms of cardiac chaos and its recession in heart failure; indeed abnormalities in left ventricular and autonomic system functions may all contribute to a decrease in complexity of the heartbeat nonlinear dynamics in CHF patients[22]. Nevertheless, of all the subjects tested, only one CHF patient failed both diagnostic criteria, corresponding to a type-I and type-II diagnostic error of 9% and 0%, respectively. Such remarkable consistency of the chaotic tests, together with the efficiency of the computational algorithm, suggest that such indices of chaos may be used as a specific, non-invasive and on-line diagnostic test for heart disease, and a possible indicator of imminent ventricular fibrillation[26]. □

Received 20 May; accepted 1 August 1997.

1. Smith, J. M. & Cohen, R. J. Simple finite-element model accounts for wide range of cardiac dysrhythmias. *Proc. Natl Acad. Sci. USA* **81,** 233–237 (1984).
2. Chialvo, D. R. & Jalife, J. Nonlinear dynamics of cardiac excitation and impulse propagation. *Nature* **330,** 749–752 (1987).
3. Chialvo, D. R., Gilmour, R. F. & Jalife, J. Low-dimensional chaos in cardiac tissue. *Nature* **343,** 653–657 (1990).
4. Jalife, J. *Ann. NY Acad. Sci.* **591** (1990).
5. Davidenko, J. M., Pertsov, R. S., Baxter, W. & Jalife, J. Stationary and drifting spiral waves of excitation in isolated cardiac muscle. *Nature* **355,** 349–351 (1989).
6. Winfree, A. T. Electrical turbulence in three-dimensional heart muscle. *Science* **266,** 1003–1006 (1994).
7. Glass, L. Dynamics of cardiac arrhythmias. *Phys. Today* 40–45 (1996).
8. Goldberger, A. L. Is the normal heartbeat chaotic or homeostatic? *News Physiol. Sci.* **6,** 87–91 (1991).
9. Sugihara, G., Allan, W., Sobel, D. & Allan, K. D. Nonlinear control of heart rate variability in human infants. *Proc. Natl Acad. Sci. USA* **93,** 2608–2613 (1996).
10. Denton, T. A., Diamond, G. A., Helfant, R. H., Khan, S. & Karagueuzian, H. Fascinating rhythm: A primer on chaos theory and its application to cardiology. *Am. Heart J.* **120,** 1419–1440 (1990).
11. Skinner, J. E., Goldberger, A. L., Mayer-Kress, G. & Ideker, R. E. Chaos in the heart: Implications for clinical cardiology. *Biotechnology* **8,** 1018–1024 (1990).
12. Goldberger, A. L. Nonlinear dynamics for clinicians: Chaos theory, fractals and complexity at the bedside. *Lancet* **347,** 1312–1314 (1996).
13. Garfinkel, A., Spano, M. L., Ditto, W. L. & Weiss, J. N. Controlling cardiac chaos. *Science* **257,** 1230–1235 (1992).
14. Garfinkel, A., Weiss, J. N., Ditto, W. L. & Spano, M. L. Chaos cotnrol of cardiac arrhythmias. *Trends Cardiovasc. Med.* **5,** 76–80 (1995).
15. Kaplan, D. T. & Cohen, R. J. Is fibrillation chaos? *Circ. Res.* **67,** 886–892 (1990).
16. Kanters, J. K., Holstein-Rathlou, N.-H. & Agner, E. Lack of evidence for low-dimensional chaos in heart rate variability. *J. Cardiovasc. Electrophysiol.* **5,** 591–601 (1994).
17. Turcott, R. G. & Teich, M. C. Fractal character of the electrocardiogram: Distinguishing heart-failure and normal patients. *Ann. Biomed. Eng.* **24,** 269–293 (1996).
18. Glass, L. Is cardiac chaos normal or abnormal? *J. Cardiovasc. Electrophysiol.* **1,** 481–482 (1990).
19. Barahona, M. & Poon, C.-S. Detection of nonlinear dynamics in short, noisy time series. *Nature* **381,** 215–217 (1996).
20. Peng, C. K., Havlin, S., Stanley, H. E. & Goldberger, A. L. Quantification of scaling exponents and crossover phenomena in nonstationary heartbeat time series. *Chaos* **5,** 82–87 (1995).
21. Ivanov, P. C. *et al.* Scaling behaviour of heartbeat intervals obtained by wavelet-based time-series analysis. *Nature* **383,** 323–327 (1996).
22. Goldberger, A. L., Rigney, D. R., Mietus, J., Antman, E. W. & Greenwald, S. Nonlinear dynamics in sudden cardiac death syndrome: heartrate oscillations and bifurcations. *Experientia* **44,** 983–987 (1988).
23. Casolo, G., Balli, E., Taddei, T., Amuhasi, J. & Gori, C. Decreased spontaneous heart rate variability on congestive heart failure. *Am. J. Cardiol.* **64,** 1162–1167 (1989).
24. Grebogi, C., Ott, E., Pelikan, S. & Yorke, J. A. Strange attractors that are not chaotic. *Physica D* **13,** 261–268 (1984).
25. Pomeau, Y. & Manneville, P. Intermittent transition to turbulence in dissipative dynamical systems. *Commun. Math. Phys.* **74,** 189–197 (1980).
26. Skinner, J. E., Pratt, C.-M. & Vybiral, T. A. Reduction in the correlation dimension of heartbeat intervals precedes imminent ventricular fibrillation in human subjects. *Am. Heart J.* **125,** 731–743 (1993).

Acknowledgements. We thank A. L. Goldberger and R. G. Mark for discussions and comments on the manuscript, and A. L. Goldberger and J. E. Mietus for providing the heartbeat data. This work was supported by grants from the National Heart, Lung and Blood Institute, National Science Foundation, and Office of Naval Research.

Correspondence and requests for materials should be addressed to C.-S.P. (e-mail: cpoon@mit.edu).

A specific neural substrate for perceiving facial expressions of disgust

M. L. Phillips*, A. W. Young†, C. Senior*, M. Brammer‡, C. Andrew§, A. J. Calder†, E. T. Bullmore‡, D. I. Perrett‖, D. Rowland‖, S. C. R. Williams§, J. A. Gray¶ & A. S. David*

** Department of Psychological Medicine, King's College School of Medicine and Dentistry and Institute of Psychiatry, 103 Denmark Hill, London SE5 8AZ, UK*
† Applied Psychology Unit, 15 Chaucer Road, Cambridge CB2 2EF, UK
§ Neuroimaging Unit, ‡ Brain Image Analysis Unit, ¶ Department of Psychology, Institute of Psychiatry, De Crespigny Park, London SE5 8AF, UK
‖ School of Psychology, University of St Andrews, Fife KY16 9JU, UK

Recognition of facial expressions is critical to our appreciation of the social and physical environment, with separate emotions having distinct facial expressions[1]. Perception of fearful facial expressions has been extensively studied, appearing to depend upon the amygdala[2–6]. Disgust—literally 'bad taste'—is another important emotion, with a distinct evolutionary history[7], and is conveyed by a characteristic facial expression[8–10]. We have used functional magnetic resonance imaging (fMRI) to examine the neural substrate for perceiving disgust expressions. Normal volunteers were presented with faces showing mild or strong disgust or fear. Cerebral activation in response to these stimuli was contrasted with that for neutral faces. Results for fear generally confirmed previous positron emission tomography findings of amygdala involvement. Both strong and mild expressions of disgust activated anterior insular cortex but not the amygdala; strong disgust also activated structures linked to a limbic cortico–striatal–thalamic circuit. The anterior insula is known to be involved in responses to offensive tastes. The neural response to facial expressions of disgust in others is thus closely related to appraisal of distasteful stimuli.

We aimed to demonstrate distinct neural substrates for perception of two emotions, fear and disgust, replicating previous observations of a link between fear perception and amygdala activation[5,6], and examining the substrate for perception of disgust. It was postulated that perception of facial expressions of disgust would involve structures implicated in the appreciation of offensive stimuli. A cortico–striatal–thalamic circuit has been identified in primates[11], which may be involved in responses to emotive stimuli. There is clinical evidence for the probable involvement of some of these structures in appreciation of disgust: impaired recognition of disgust from facial expressions has been reported both in patients with symptomatic Huntington's disease[12], and presymptomatic carriers of the Huntington's gene[13].

Subjects viewed grey-scale pictures of faces from a standard set[14] depicting disgusted, fearful and neutral expressions. There were two levels of intensity (75 and 150%) for the facial expressions of disgust and fear for each individual face, and one level for the neutral expression, all produced by computer graphical manipulation of the prototype of each expression[15] (Fig. 1). As a neutral face, we used an image with a slightly (25%) happy expression (see Methods). Subjects viewed blocks of emotional (disgusted or fearful) faces alternating with neutral faces in blocks. There were four separate experiments, in a randomized order, incorporating an alternating (neutral/emotional) design for each emotion (fear/disgust) and intensity of expression (mild, 75%; strong, 150%). After presentation of each face, subjects made a decision as to its sex by pressing one of two buttons with the right thumb. The sex decision task was chosen to allow an identical task and response across all conditions, and to permit comparison to a previous study of fear which also

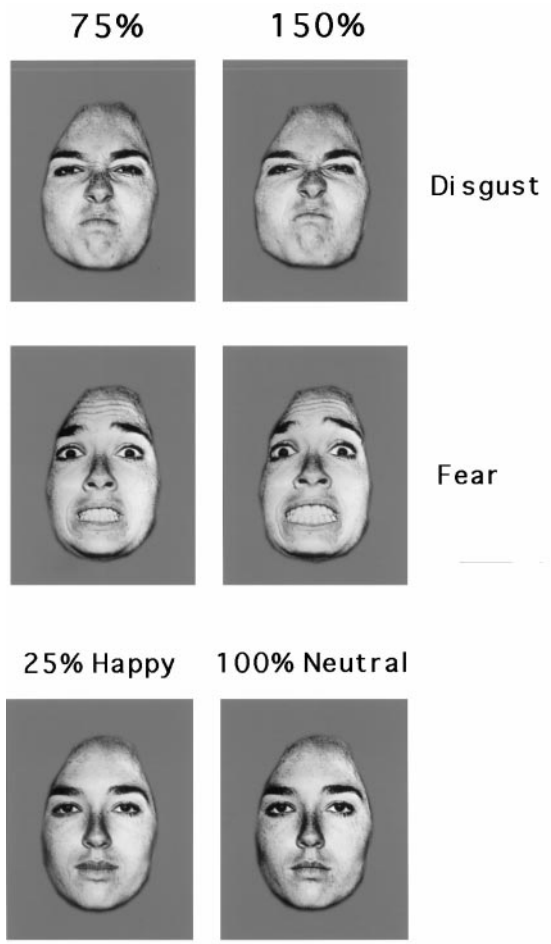

Figure 1 Faces from a standard set[14] were computer-transformed[15] to create two levels of intensity of expressed fear and disgust. Examples of faces depicting 100% neutral, 75 and 150% disgust, and 75 and 150% fear are demonstrated, together with an example of a stimulus depicting a mildly happy expression (75% neutral and 25% happy) which was used as the neutral baseline.

Table 1 Main activated brain regions in the different experiments

BA/region	Side	Tal. x*	Tal. y*	Tal. z*	No activated voxels
(a) 75% Fearful faces versus neutral faces					
Insula	L	–40	–25	4	8†
Amygdala	L	–26 –26	–14 –6	–13 –7	3† 1†
(b) 150% Fearful faces versus neutral faces					
Putamen	R	23 29	8 11	–7 20	7† 5†
Amygdala	R	20	–11	–13	4‡
(c) 75% Disgusted faces versus neutral faces					
Anterior-mid Insula	R	35 38	–11 –6	–2 4	5† 3†
32/Medial frontal cortex	R	17	39	9	5†
(d) 150% Disgusted faces versus neutral faces					
32/Medial frontal cortex	L	–3	42	15	14†
18/Peristriate cortex	L	–14	–72	–7	11†
Anterior insula	R L	35 46 –32	31 11 22	9 9 15	10† 8† 6†
23/Posterior cingulate cyrus	R	3	–53	15	8†
46/Dorsolateral prefrontal cortex	R	35	42	15	7†
19/Parastriate cortex	R	29	–75	15	5†
Thalamus	R	26	–31	15	5†
37/Inferior–posterior temporal cortex	L	–26 –40	–50 –47	–7 –7	5† 4†
22/Superior temporal cortex	L	–43	–36	15	4†
21/Middle temporal cortex	R	46	–28	–2	4†
Putamen	R	23	3	9	4†
(e) Regions with significantly different activation for 150% versus 75% disgust					
Anterior insula	R	38	17	9	16†
18/Peristriate cortex	L	–20	–72	–7	8†

* Talairach co-ordinates refer to the voxel with the maximum FPQ (fundamental power quotient) in each regional cluster.
† Probability of false activation of each voxel in the generic brain map over all seven subjects was 0.004.
‡ Probability of false activation of each voxel in the amygdala region of interest over all seven subjects was 0.02.

used this procedure[6]. We assumed (and our data confirm) that there would be a neural response to the face's displayed emotion even though subjects were not explicitly asked about it. Subjects were not informed that the aim of the study was to investigate responses to emotional expression.

Activation was demonstrated in the left amygdala for perception of fearful facial expression at the 75% intensity level with a voxel-wise probability of type I (false-positive) error $P < 0.004$. At this level of significance testing, we expect less than 6 false-positive voxels in a slice of the image comprising about 1,500 voxels in total. At the 150% level of fearful expression, we could not demonstrate activation of the amygdala at this relatively conservative level of significance testing. As the amygdala has been shown to be responsive to fear in other studies, we adopted a region of interest approach to analysis of these data. We tested the 18 voxels representing the amygdala complex bilaterally, with voxel-wise probability of type I error $P < 0.02$; at this level, we expect less than one false-positive voxel in the right and left amydala regions. This approach demonstrated significant activation in the right amygdala for perception of 150% fearful facial expression (see Table 1a, b for details of generic brain activation foci in response to fearful facial expression). The lack of a dose-response effect for perception of fearful facial expression is discussed below.

The principal focus of interest in our study was the neural response to facial expressions of disgust. The most striking finding for perception of facial expressions of disgust was activation in the right insula ($P < 0.004$), but not the amygdala (Table 1c, d and Fig. 2). Activation in the right anterior insula was significantly greater ($P < 0.004$) for perception of the 150% compared with the 75% disgust intensity (Table 1e and Fig. 3).

We have demonstrated a neural substrate for perception of facial expressions of disgust involving primarily the anterior insula, but, unlike fear, not the amygdala. The anterior insula is connected to the ventro–posterior–medial thalamic nucleus, and has been identified in primates as gustatory cortex[16], containing neurons that respond to pleasant and unpleasant tastes[17]. In humans, anterior insula activation has been demonstrated while tasting salt in a functional imaging study[18]. Insula activation has also been demonstrated during perception of aversive stimuli such as pain[19]. Activation of the anterior insula during perception of facial expressions of disgust suggests that appreciation of visual stimuli depicting other's disgust is closely linked to the perception of unpleasant tastes and smells[8]. We also demonstrated activation in medial frontal cortex (Brodmann area 32, BA 32), anatomically connected with orbitofrontal cortex[20], during appreciation of both intensities of disgust, and in the right putamen and thalamus for the higher intensity of disgust. The emotional response to visceral, offensive stimuli may involve a limbic circuit connecting orbitofrontal cortex with ventral striatum

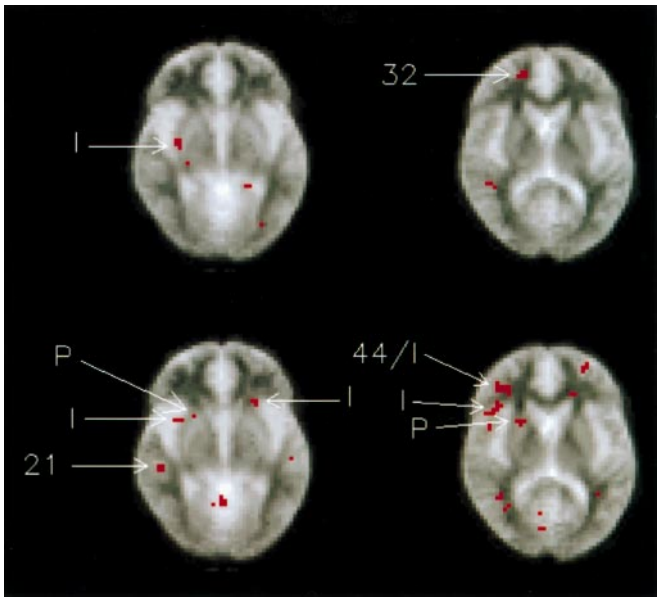

Figure 2 Generic brain activations in seven right-handed normal subjects during perception of faces depicting 75% (top row) and 150% (bottom row) disgust intensity. The grey-scale template was calculated by voxel-by-voxel averaging of the individual EPI images of all subjects, following transformation into Talairach space. The transverse sections in each experiment are at 2 mm below (left) and 9 mm above (right) the AC-PC line (right side of the brain on the left side of each section, and vice versa). Major regions of activation (probability of false activation <0.004) for perception of faces depicting 75% disgust versus a neutral expression are demonstrated in the right insula (I) and right medial frontal cortex (BA 32); those for faces depicting 150% disgust versus a neutral expression are demonstrated in the right and left anterior insula (I), right anterior insula bordering on inferior frontal cortex (BA 44), right putamen (P), and right middle temporal gyrus (BA 21).

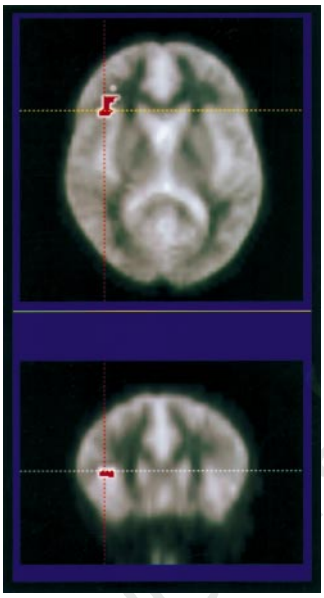

Figure 3 The difference image demonstrating significant ($P < 0.004$) differences in activation for perception of faces depicting 150% intensity of disgust (versus a neutral expression) and faces depicting 75% intensity of disgust (versus a neutral expression). The grey-scale template was as for Fig. 2. The largest region of activation was in the right anterior insula (Talairach coordinates 38, 17, 9), with twice the number of activated voxels compared with other regions of the difference image. Transverse ($z = 9$) and coronal ($y = 17$) sections are shown depicting this activation in the right insula.

and the mediodorsal thalamic nucleus[11]. Our results suggest that structures linked with this circuit are involved in perception of facial expressions of disgust. Activation of posterior cingulate and visual cortex (Table 1d, e) may relate to arousal by an emotive visual stimulus[21].

Unlike previously reported positron emission tomography (PET) findings[6], there was no dose-response effect for amygdala activation with intensity of fearful facial expression. The time parameters differed between the PET study and our fMRI study; furthermore, a previous fMRI study has demonstrated rapid within-experiment habituation of amygdala response[5], which could weaken the total extent of amygdala activation during the course of a five-minute experiment.

During the experimental procedure, subjects may have merely mimicked the facial expressions, rather than recognized the emotion depicted. As there was no activation demonstrated in the supplementary motor area, involved in movements of the mouth[22], for any of the four experiments, this explanation for our results is unlikely.

The results demonstrate for the first time evidence for a differentiation between the neural responses to facial expressions of two negative emotions, fear and disgust. Disgust can be considered to be a response that evolved to lead to avoidance of contamination by offensive stimuli, and in particular, avoidance of ingestion of potentially harmful (for example, decayed) food[8]. We have demonstrated activation of the anterior insula, with its identified role as gustatory cortex, during appreciation of visual stimuli depicting expressions of disgust. Perception of others' disgust and that of taste appear, therefore, to have a similar neural substrate. It is interesting that the neural response to facial expressions of disgust in others should be linked to brain regions involved in gustatory responses. This suggests that our responses to others' disgust have, perhaps through associative learning between visual stimuli and taste[23], become closely linked to the appraisal of distasteful stimuli. □

Methods

Subjects. Seven right-handed healthy volunteers (five female and two male; mean age, 27 years; mean IQ estimate, 115) participated in the study. Exclusion criteria included history of brain injury and past and current psychiatric illness. No subject was taking regular medication.

Experimental design. Subjects participated in four 5-min experiments for presentation of emotional versus neutral facial stimuli. The faces of eight individuals (three male and five female) from a standard set of 'prototype' expressions of emotion[14] were computer-transformed[15] to create two levels of intensity of expressed fear and disgust (Fig. 1). At 75% intensity, the image was positioned with its features 75% along the continuum from neutral to the disgust prototype, or from neutral to the fear prototype. At 150% intensity, differences between the locations of facial features in the fear or disgust prototypes and a neutral expression were exaggerated by 50%. Studies of normal subjects have found that 150% images are recognized faster than 75% images for facial expressions of all basic emotions, showing the efficacy of this procedure in enhancing perceived emotion[24]. In view of the fact that 100% neutral (muscles relaxed) faces from the standard set can appear slightly cold and threatening because it is conventional to signal approval in normal social interaction, we used as the neutral baseline stimulus a very slightly happy expression (75% neutral, 25% happy; Fig. 1). To familiarize subjects with the stimuli, they viewed all faces once, each presented for 3 s on a portable computer screen. In each experiment, the eight different faces depicting the same emotion and intensity of expression were presented one at a time on a computer screen in randomized order for 3 s each, followed by a 0.75-s interval in which the screen was blank. This was followed by presentation of eight neutral faces of the same eight individuals in a similar way. Stimuli were presented 3.5 m from the subject, subtending visual angles of ten degrees horizontally and eight degrees vertically. Each experiment comprised ten separate 30-s presentation phases, alternating between emotional (phase A) and neutral (phase B) stimuli, with the first presentation, either emotional (A) or neutral (B), counterbalanced across experiments for each subject, and also across subjects. The presentation order of the four experiments was also counterbalanced across subjects. Subjects made a decision as to the sex of each face by pressing one of two buttons with the right thumb. To allow for practice with the button box, subjects were presented with eight 100% neutral faces before each of the four different experiments. Accuracy of judgement of

sex for all faces by the seven subjects was near 100% (mean response over all subjects and experiments: 96.6%, range: 81.3–100%).

Image acquisition and analysis. Echoplanar MR brain images were acquired using a 1.5 Tesla GE Signa system (General Electric) retrofitted with advanced NMR hardware (ANMR) using a standard head coil. 100 T2*-weighted images depicting BOLD contrast[25] were acquired over 5 min (for each experiment) at each of 14 near-axial non-contiguous 5-mm-thick planes parallel to the intercommissural (AC-PC) line, providing whole-brain coverage: TE, 40 ms; TR, 3 s; in-plane resolution, 3 mm; interslice gap, 0.5 mm. An inversion recovery EPI dataset was also acquired at 43 near-axial 3-mm-thick planes parallel to the AC-PC line: TE, 80 ms; TI, 180 ms; TR, 16 s; in-plane resolution, 3 mm; number of signal averages, 8. The periodic change in T2*-weighted signal intensity at the (fundamental) experimentally determined frequency of alternation between A and B conditions was analysed by pseudogeneralized least-squares (PGLS) fit of a sinusoidal regression model to the movement-corrected[26] time series at each voxel, yielding parametric maps of the squared amplitude of the response at the stimulus frequency divided by its standard error—the fundamental power quotient, FPQ (ref. 27). Each observed time series was randomly permuted ten times, and FPQ estimated as above in each randomized time series, to generate 10 randomized parametric maps of FPQ for each subject in each anatomical plane. To construct generic brain activation maps, showing brain regions activated over a group of subjects, observed and randomized parametric maps of FPQ estimated in each individual were first transformed into the stereotactic space of Talairach and Tournoux and smoothed by a gaussian filter with full width at half maximum of 11 mm (ref. 28). The median observed value of FPQ was then computed at each voxel in standard space and its statistical significance tested by reference to the null distribution of median FPQ computed from the identically smoothed and spatially transformed randomized maps. For a one-tailed test of size p, the critical value was the $100^{*}(1-p)$th percentile of the randomization distribution[29]. To identify voxels that demonstrated significant difference in standardized power of response to faces that expressed disgust with different intensities, the observed difference in median FPQ between these two experimental conditions was computed at each voxel. Subjects were then randomly reassigned to one of two equal-sized groups and the difference in median FPQ between randomized groups was computed at each voxel[30]. This process was repeated 64 times and the results were pooled over voxels to generate a null distribution for difference in median FPQ. For a two-tailed test of size p, the critical values were the $100^{*}(1-p/2)$th and $100^{*}(p/2)$th percentiles of the randomization distribution.

Received 26 March; accepted 8 July 1997.

1. Ekman, P. An argument for basic emotions. *Cog. Emot.* **6,** 169–200 (1992).
2. Adolphs, R. *et al*. Impaired recognition of emotion in facial expressions following bilateral damage to the human amygdala. *Nature* **372,** 669–672 (1994).
3. Adolphs, R. *et al*. Fear and the human amygdala. *J. Neurosci.* **16,** 7678–7687 (1995).
4. Calder, A. J. *et al*. Facial emotion recognition after bilateral amygdala damage: differentially severe impairment of fear. *Cogn. Neuropsychol.* **13,** 699–740 (1996).
5. Breiter, H. C. *et al*. Response and habituation of the human amygdala during visual processing of facial expression. *Neuron* **17,** 875–887 (1996).
6. Morris, J. *et al*. A differential neural response in the human amygdala to fearful and happy facial expressions. *Nature* **383,** 812–815 (1996).
7. Darwin, C. *The Expression of the Emotions in Man and Animals* (University of Chicago Press, Chicago, 1965).
8. Rozin, P. & Fallon, A. E. A perspective on disgust. *Psychol. Rev.* **94,** 23–41 (1987).
9. Rozin, P., Lowery, L. & Ebert, R. J. Varieties of disgust faces and the structure of disgust. *Pers. Soc. Psychol.* **66,** 870–881 (1994).
10. Vrana, S. R. The psychophysiology of disgust: differentiating negative emotional context with facial EMG. *Psychophysiology* **30,** 279–286 (1993).
11. Alexander, G. E. *et al*. Parallel organizaiton of functionally segregated circuits linking basal ganglia and cortex. *Annu. Rev. Neurosci.* **9,** 357–381 (1986).
12. Sprengelmeyer, R. *et al*. Perception of faces and emotions: loss of disgust in Huntington's disease. *Brain* **119,** 1647–1665 (1996).
13. Gray, J. M. *et al*. Impaired recognition of disgust in Huntington's disease gene carriers. *Brain* (in the press).
14. Ekman, P. & Friesen, W. V. *Pictures of Facial Affect* (Consulting Psychologists, Palo Alto, 1976).
15. Perrett, D. I., May, K. A. & Yoshikawa, S. Facial shape and judgements of female attractiveness. *Nature* **368,** 239–242 (1994).
16. Rolls, E. T. in *Handbook of Clinical Olfaction and Gustation* (ed. Doty, R. L.) (Dekker, New York, 1994).
17. Yaxley, S. *et al*. The responsiveness of neurons in the insular gustatory cortex of the macaque monkey is independent of hunger. *Physiol. Behav.* **42,** 223–229 (1988).
18. Kinomura, S. *et al*. Functional anatomy of taste perception in the human brain studied with positron emission tomography. *Brain Res.* **659,** 263–266 (1994).
19. Casey, K. L. *et al*. Positron emission tomographic analysis of cerebral structures activated specifically by repetitive noxious heat stimuli. *J. Neurophysiol.* **71,** 802–807 (1994).
20. Barbas, H. Organization of cortical afferent input to orbitofrontal areas in the Rhesus monkey. *Neuroscience* **56,** 841–864 (1993).
21. Kosslyn, S. M. *et al*. Neural effects of visualizing and perceiving aversive stimuli: a PET investigation. *NeuroReport* **7,** 1569–1576 (1996).
22. Gentilucci, M. *et al*. Functional organization of inferior area 6 in the macaque monkey: I. Somatotopy and the control of proximal movements. *Exp. Brain Res.* **71,** 475–490 (1988).
23. Rolls, E. T. *et al*. Orbitofrontal cortex neurons: Role in olfactory and visual association learning. *J. Neurophysiol.* **75,** 1970–1981 (1996).
24. Calder, A. J., Young, A. W., Rowland, D. & Perrett, D. I. Computer-enhanced emotion in facial expressions. *Proc. R. Soc. B.* (in the press).
25. Ogawa, S., Lee, T. M., Kay, A. R. & Tank, D. W. Brain magnetic resonance imaging with contrast dependent blood oxygenation. *Proc Natl Acad. Sci. USA* **87,** 8868–8872 (1990).
26. Friston, K. J. *et al*. Movement-related effects in fMRI time series. *Mag. Res. Med.* **35,** 346–355 (1996).
27. Bullmore, E. T. *et al*. Statistical methods of estimation and inference for functional MR image analysis. *Mag. Res. Med.* **35,** 261–277 (1996).
28. Talairach, J. & Tournoux, P. *Co-planar Stereotactic Atlas of the Human Brain* (Thieme, Stuttgart, 1988).
29. Brammer, M. J. *et al*. Generic brain activation mapping in fMRI: a nonparametric approach. *Mag. Res. Imag.* (in the press).
30. Edgington, E. S. *Randomisation Tests* (Dekker, New York, 1980).

Acknowledgements. M.L.P. is supported by an MRC clinical training fellowship; E.T.B. is supported by the Wellcome Trust. We thank H. Critchley for advice and for comments on the manuscript, and A. Simmons for technical support.

Correspondence and requests for materials to M.L.P. (e-mail: spmamlp@iop.bpmf.ac.uk).

Transmissions to mice indicate that 'new variant' CJD is caused by the BSE agent

M. E. Bruce*, R. G. Will†, J. W. Ironside†, I. McConnell*, D. Drummond*, A. Suttie*, L. McCardle†, A. Chree*, J. Hope‡, C. Birkett‡, S. Cousens§, H. Fraser* & C. J. Bostock‡

** Institute for Animal Health, BBSRC/MRC Neuropathogenesis Unit, West Mains Road, Edinburgh EH9 3JF, UK*
† National CJD Surveillance Unit, Western General Hospital, Edinburgh EH4 2XU, UK
‡ Institute for Animal Health, Compton, Newbury, Berkshire RG20 7NN, UK
§ Department of Epidemiology and Population Science, London School of Hygiene and Tropical Medicine, London WC1E 7HT, UK

There are many strains of the agents that cause transmissible spongiform encephalopathies (TSEs) or 'prion' diseases. These strains are distinguishable by their disease characteristics in experimentally infected animals, in particular the incubation periods and neuropathology they produce in panels of inbred mouse strains[1–4]. We have shown that the strain of agent from cattle affected by bovine spongiform encephalopathy (BSE) produces a characteristic pattern of disease in mice that is retained after experimental passage through a variety of intermediate species[5–7]. This BSE 'signature' has also been identified in transmissions to mice of TSEs of domestic cats and two exotic species of ruminant[6,8], providing the first direct evidence for the accidental spread of a TSE between species. Twenty cases of a clinically and pathologically atypical form of Creutzfeldt–Jakob disease (CJD), referred to as 'new variant' CJD (vCJD)[9], have been recognized in unusually young people in the United Kingdom, and a further case has been reported in France[10]. This has raised serious concerns that BSE may have spread to humans, putatively by dietary exposure. Here we report the interim results of transmissions of sporadic CJD and vCJD to mice. Our data provide strong evidence that the same agent strain is involved in both BSE and vCJD.

Transmissions to mice were set up from six typical sporadic cases of CJD (spCJD) and three cases of vCJD. All were homozygous for methionine at codon 129 of the 'prion protein' (PrP) gene, and none carried PrP gene mutations associated with familial disease. The spCJD cases included two dairy farmers (aged 61 and 64 years) who had had BSE in their herds and had therefore been potentially exposed to BSE-infected cattle or contaminated animal feed[11]; two 'contemporary' cases (aged 55 and 57 years) with no known occupational exposure to BSE; and two 'historical' cases (aged 57 and 82 years) who had died in 1981 and 1983, before the onset of the